PCCP

Accepted Manuscript

ROYAL SOCIETY OF CHEMISTRY

www.rsc.org/pccp

Journal Name

RSCPublishing

ARTICLE

Vibrational Properties and Specific Heat of Core-Shell Ag-Au Icosahedral Nanoparticles

Cite this: DOI: 10.1039/xoxxoooooox

Huziel E. Sauceda[a] and Ignacio L. Garzón[a]

Received ooth January 2012,
Accepted ooth January 2012

DOI: 10.1039/xoxxoooooox

www.rsc.org/

The vibrational density of states (VDOS) of metal nanoparticles can be a fingerprint of their geometrical structure and determine their low-temperature thermal properties. Theoretical and experimental methods are available nowadays to calculate and measure it over a size range of 1 – 4 nm. In this work, we present theoretical results on the VDOS of Ag-Au icosahedral nanoparticles with core-shell structure in that size range (147-923 atoms). Results are obtained by changing the size and type of atoms in the core-shell structure. For all sizes investigated, it is obtained a smooth and monotonic variation of the Ag to the Au VDOS by increasing the number of core Au atoms and vice versa. Nevertheless, the $Ag_{561}Au_{362}$ nanoparticle, with Ag core, shows an anomalous enhancement at low frequencies. An analysis of the calculated VDOSs indicates that as a general trend the low-frequency region is mainly due to the shell contribution, whereas at high frequencies the core effect would be dominant. A linear variation with size is obtained for the period of the quasi-breathing mode (QBM), in agreement with the behaviour obtained for pure Ag and Au nanoparticles. A non-monotonic variation is obtained for the QBM frequency as a function of the Ag concentration for all nanoparticles investigated. The calculated specific heat at low temperatures of the Ag-Au nanoparticles is smaller (larger) than the corresponding one for the pure Au (Ag) nanoparticles of the same size. Nevertheless, the VDOS enhancement at low frequencies of the $Ag_{561}Au_{362}$ nanoparticle with Ag core, induced larger values of the specific heat with respect to that one of the pure Au_{923} nanoparticle in the temperature range of 5-15 K.

Introduction

Nanoalloys are an interesting phase of matter at the nanoscale not only due to their finite size and peculiar morphologies, but also because they have composition-dependent physicochemical properties, with potential applications in several areas of Nanotechnology.[1,2] Structural, electronic, optical, thermal (melting), and catalytical properties have been widely investigated both theoretically[2,3] and experimentally.[2,4] On the other hand, vibrational properties studies on nanoalloys are scarce, although some experimental[5-8] and theoretical[7-9] studies on specific bimetallic nanoparticles have been reported. For example, the influence of size, composition, and chemical order on the vibrational properties of gold-silver nanolloys was theoretically investigated using an atomistic description based on a many-body potential to model the metal atom interactions.[9] As a general conclusion, it was found that the vibrational properties of these bimetallic nanoparticles depend on size, composition, and chemical ordering in nontrivial ways.[9]

In this work, we theoretically investigate how would change the vibrational properties of a metal nanoparticle when a second metal is incorporated into the structure of the first one. Our study will focus on the calculation of the nanoalloy vibrational density of states (VDOS). This quantity, providing information on the whole vibrational frequency spectrum, is considered a fingerprint of the nanoparticle structure since it allows its structural determination, after a comparison with experimental measurements of it.[10] In fact, in a recent study performed by us,[10] it was proposed the structural determination of Ag and Au nanoparticles from the comparison of the

calculated VDOS with those measured using plasmon resonance Raman scattering.[11,12] In this case, the results indicated that most of the Ag and Au nanoparticles, with average size ~ 5 nm, in the experimental samples should have icosahedral structures.[10] In other investigations, we have studied the size and shape dependence, as well as the evolution towards bulk behaviour of the VDOS of pure metal nanoparticles.[13,14] These studies showed the importance of the VDOS as a useful quantity to describe the vibrational behaviour of metal nanoparticles, motivating the extension of such calculations to bimetallic nanoparticles.

One of the vibrational modes of a special interest is the quasi-breathing one (QBM) since it can be correlated with a nanoparticle radial volume change. Moreover, the QBM period has been measured through the relative optical transmission change using pump-probe spectroscopy.[15] A linear variation with size was obtained, both theoretically and experimentally, for the QBM period of pure Pt and Au nanoparticles.[13,15] A similar behaviour was obtained from the calculation of the QBM period for $(Ag_{0.5}\text{-}Au_{0.5})_n$, n=147-3871, with core-shell and alloy structures, whereas a nonlinear variation of the QBM frequency was calculated by changing the relative composition of the bimetallic nanoparticle.[9] In order to gain additional insights into the size and composition dependence of the QBM frequency, in this work, we also perform a systematic study of this quantity for icosahedral core-shell Ag-Au nanoparticles.

The calculation of thermal properties at low temperatures, like the specific heat, is another advantage of the availability of the nanoparticle VDOS.[14,16] These studies have shown that there is a small variation with size and shape for the specific heat of pure Au nanoparticles in the size range of 0.5 – 4 nm. An interesting question would be to investigate the dependence of the specific heat with size and composition of bimetallic nanoparticles. In this work, we also address this issue.

To make a systematic study of the vibrational and thermal properties of bimetallic nanoparticles, we fix the material, structure, and type of segregation by considering Ag-Au core-shell icosahedral nanoparticles. For these bimetallic nanoparticles, it is calculated the VDOS for four different sizes with a total number of atoms: 147, 309, 561, and 923. In each case, the core size is changed from 13 up to 561 considering either Ag or Au atoms. This theoretical study would be relevant since it has been already reported the synthesis by chemical or electrochemical deposition of $Ag_{core}\text{-}Au_{shell}$ and $Ag_{shell}\text{-}Au_{core}$ nanoparticles.[17-20] In fact, it is expected that the present theoretical study would motivate the extension of experimental optical[17,20,21] measurements to vibrational ones.

Theoretical background

To model the metallic bonding in the nanoalloys we consider the many-body Gupta potential, which is based on the second-moment approximation to a tight binding theory.[22-24] The parameters of the Gupta potential used here are shown in the Supporting Information (SI) section. Their values are similar to those obtained by fitting to experimental properties of bulk metals and alloys.[25,26] This semiempirical potential has been extensively utilized to study structural, dynamical, and thermal (melting) properties of Ag-Au nanoalloys.[25-30] As a matter of fact, the reliability of this semiempirical approach to model the atomic interaction in Ag-Au bimetallic nanoparticles has been shown after the agreement obtained with the geometries of clusters larger than 24 atoms calculated with density functional theory.[30]

The vibrational frequencies of the nanoalloys were calculated within the harmonic approximation by a diagonalization of the Hessian matrix.[10,13,14,16] The second derivatives of the Gupta potential were evaluated at the

equilibrium atomic positions, which were calculated by doing simulated quenching through constant-energy molecular dynamics and conjugate gradient relaxations on the potential energy surface.[31-33] Core-shell Mackay icosahedral geometries were used for the local structural relaxations. The VDOS was constructed using a Gaussian broadening (with a width of 1.9 cm^{-1}) of the 3*N*-6 vibrational frequencies. To locate the frequency of the QBM, a method described in Ref. 13 for pure nanoparticles was implemented in the present case. Once the vibrational frequencies were available, the specific heat was calculated from the quantum mechanical expression for a set of 3*N*-6 independent harmonic oscillators.[14,16]

Results and discussion

Figure 1 displays the VDOS for the 923-atom bimetallic icosahedral Ag-Au nanoparticles with different core-shell compositions. In the left panels (from top to bottom), it can be seen a smooth and monotonic variation of the VDOS going from the pure Au_{923} nanoparticle to the Ag_{923} one, by decreasing the size of the Au core. A similar variation is shown in the right panels for the opposite case where the Ag core decreases in size. A more careful analysis of the VDOSs displayed in Fig. 1 indicates that as a general trend the low-frequency region is mainly due to the shell contribution, whereas at high frequencies the core effect would be dominant. Interestingly, this behaviour has been also found for pure metal FCC and icosahedral nanoparticles.[34] In fact, for the Au_{core}-Ag_{shell} nanoparticles, the low-frequency region of their VDOS (see left panels of Fig. 1) looks very similar to the Ag_{923} VDOS one, as the size of the Ag shell increases. On the other hand, the high frequency region only shows a small and continuous blue shift, and the absence of the high frequency tail even for the case of the smaller Au core in the $Au_{13}Ag_{910}$ nanoparticle. Instead, this high frequency tail, with modes around 250 cm^{-1}, is present in all Ag_{core}-Au_{shell} nanoalloys (see right panels of Fig. 1) resembling the case of the Ag_{923} pure nanoparticle. At this point, it is useful to recall that the high frequency modes in the icosahedral Ag_{923} nanoparticle correspond to vibrations of the inner Ag_{13} core.[10,13,14] The dominant behaviour of the shell contribution from the Au atoms to the low-frequency region of the VDOS can also be observed in the right panels of Fig. 1 as the size of shell grows in the Ag_{core}-Au_{shell} nanoalloys.

A special nanoalloy, showing an anomalous behaviour at low frequencies is the $Ag_{561}Au_{362}$ nanoparticle with Ag core. Its VDOS (see the second right panel in Fig. 1) displays an enhancement (peak) at low frequencies that is not present in the other core-shell nanoparticles. This behaviour might be related with the distinct contractions of the radial distances of the Au atoms that break the icosahedral symmetry of the Au shell.

In the SI section (Figs. S1-S3) it is shown the corresponding VDOSs for the 561-, 309-, and 147-atom bimetallic nanoparticles. For these smaller nanoalloys a smooth and monotonic variation is also obtained going from the VDOS of the pure Au nanoparticle to the Ag one and vice versa. Nevertheless, since the number of atoms is smaller, the VDOSs display a more discrete peak structure. Interestingly, Figs. S1-S3 also show the anomalous enhancement at low frequencies for the $Ag_{309}Au_{252}$, $Ag_{147}Au_{162}$, and $Ag_{55}Au_{92}$ bimetallic nanoparticles with Ag core, in analogy with the $Ag_{561}Au_{362}$ nanoparticle mentioned above.

A further analysis of the calculated VDOSs can be performed by looking at the behaviour of three specific vibrational modes: the acoustic gap (lowest frequency), the cut-off (highest frequency), and the QBM. Figure 2 displays the dependence of the acoustic gap and cut-off frequencies with the composition percentage of the Ag atoms in the bimetallic nanoparticles with 923 atoms. Figure 2(a) indicates a very small variation of the cut-off frequency when the

Ag/Au (green/red lines) shell grows, confirming that at high frequencies the core contribution is dominant. On the other hand, Figure 2(b) indicates an increasing variation of the acoustic gap when the number of Ag atoms grows either in the core or in the shell of the corresponding nanoparticle. The anomalous behaviour of the $Ag_{561}Au_{362}$ nanoparticle with Ag core is also displayed in Fig. 2(b) (green line), indicating that for this nanoparticle the acoustic gap has its minimum value, with respect to those obtained for other compositions.

Figure 3 displays the variation of the QBM as a function of the composition percentage of Ag atoms for the 923-, 561-, 309, and 147-atom Ag_{core}-Au_{shell} and Au_{core}-Ag_{shell} nanoparticles. All sizes show a non-linear variation as a function of the Ag composition. These results are in overall agreement with those reported in Ref. 9. Nevertheless, differences in the numerical values of the QBM frequencies exist, that are due to the distinct methodology used to locate and calculate the frequency of this specific vibrational mode. A comparison with the present results indicates that the approximate method used in Ref. 9 overestimates the QBM frequencies by ~ 6 cm^{-1} for the 923- and 561-atom nanoalloys. Other difference between the present calculations and those reported in Ref. 9 is related with the shell structure, which in the present case corresponds to a closed one based on the Mackay icosahedra magic numbers, instead of using 10% variations in the Ag composition. A linear variation of the QBM period as a function of size is displayed in Fig. 4 for Ag_{core}-Au_{shell} and Au_{core}-Ag_{shell} nanoparticles, where only 1 and 2 closed Mackay icosahedral shells are considered. As a reference, it is also shown the results obtained for pure Ag and Au nanoparticles.[13] This linear dependence is in agreement with that one obtained in Ref. 9, and with the results calculated and measured for pure metal nanoparticles.[13] Nevertheless, it should be noticed that the Ag_{core}-Au_{shell} nanoparticles with Ag core and a single Au shell do not follow a clear linear dependence, although the QBM period increases monotonically with size. In particular, much smaller values of the QBM periods are obtained for the $Ag_{147}Au_{162}$ and $Ag_{309}Au_{252}$ nanoparticles with Ag core and one-atom width Au shell. Again, this anomalous behaviour might be due to the distinct radial contractions of the Au atoms forming the external shell.

One advantage of the availability of the VDOS is that a calculation of low-temperature thermal properties like the specific heat is straightforward.[14,16] Here, we will focus on the results for the 923-atom nanoalloys. Figure S4 in the SI section shows that the specific heat as a function of temperature of the Ag_{core}-Au_{shell} and Ag_{shell}-Au_{core} nanoalloys lies between the values of the pure Au_{923} and Ag_{923} nanoparticles. The higher values of the specific heat for the pure Au nanoparticle are explained by the larger enhancement of its VDOS at low frequencies, with respect to that one of pure Ag one, as can be seen in Fig. 1. The smooth and monotonic variation of the nanoalloys VDOSs displayed in Fig. 1 reflects in the specific heat results shown in Fig. S4. Nevertheless, the already mentioned anomalous enhancement at low frequencies displayed by the $Ag_{561}Au_{362}$ nanoparticle with Ag core, is the cause of a distinct variation of its specific heat. In fact, Fig. 5 indicates that this nanoalloy shows larger values than the pure Au nanoparticle along a temperature range between 5 and 15 K. In contrast, the $Au_{561}Ag_{362}$ nanoparticle with Au core does not show larger values than those of the Au nanoparticle, confirming the distinct effect of the Au shell at low frequencies and temperatures.

Conclusions

The vibrational properties of Ag_{core}-Au_{shell} and Au_{core}-Ag_{shell} icosahedral nanoparticles with core-shell structure in the size range of 147-923 atoms were studied using the semiempirical many-body Gupta potential. Results for the VDOS and characteristic vibrational modes (acoustic gap, QBM, and cut-off frequencies)

were obtained by changing the size and type of atoms in the core-shell structure. The main trend emerging from these calculations indicates that the low-frequency region of the VDOS is mainly due to the shell contribution, whereas at high frequencies the core effect would be dominant. This trend is in agreement with that obtained for pure metal nanoparticles.[34]

Our results also show that, in general, the change in the vibrational and low-temperature thermal properties (specific heat) of a metal nanoparticle when a second metal is incorporated into the structure of the first one is smooth and monotonic. Nevertheless, the present calculations were able to find a special nanoalloy, the $Ag_{561}Au_{362}$ nanoparticle with Ag core, that shows an anomalous enhancement in its VDOS at low frequencies. This enhancement is the cause of a higher value of its specific heat as compared with the pure Au_{923} icosahedral nanoparticles, in the range of 5-15 K.

It is expected that the present study not only motivate further theoretical studies for other types and compositions of nanoalloys, but also the performance of experimental measurements of their vibrational and low-temperature thermal properties.

Acknowledgements

We acknowledge support from Conacyt-México under Project 177981. Calculations were done using resources from the Supercomputing Center DGTIC-UNAM. HES acknowledges support from Programa de Doctores Jóvenes de la Universidad Autónoma de Sinaloa. We thank M. en C. Israel Acuña for programing in CUDA language the molecular dynamics and vibrational analysis codes used in this work.

Notes and references

[a] Instituto de Física, Universidad Nacional Autónoma de México; Apartado Postal 20-364; 01000 México, D. F.; México; Email: garzon@fisica.unam.mx; huziel@fisica.unam.mx

Electronic Supplementary Information (ESI) available: Parameters of the many-body Gupta potential, VDOSs for Ag_{core}-Au_{shell} and Au_{core}-Ag_{shell} nanoparticles with 147, 309, and 561 atoms. Specific heat for 923-atom nanoalloys with different Ag-Au relative compositions.

1. R. Ferrando, J. Jellinek and R. L. Johnston, *Chem. Rev.*, 2008, **108**, 845.
2. *Nanoalloys: From Fundamentals to Emergent Applications*, ed. F. Calvo, Elsevier, Amsterdam, 2013.
3. A. Agüado, in *Nanoalloys: From Fundamentals to Emergent Applications*, ed. F. Calvo, Elsevier, Amsterdam, 2013, p. 75.
4. S. Mejía-Rosales, A. Pomce, M. José-Yacamán, in *Nanoalloys: From Fundamentals to Emergent Applications*, ed. F. Calvo, Elsevier, Amsterdam, 2013, p. 113.
5. H. Portales, L. Saviot, E. Duval, M. Gaudry, E. Cottancin, J. Lermé, M. Pellarin, M. Broyer, B. Prével and M. Treilleux, *Eur. Phys. J. D*, 2001, **16**, 197.
6. H. Portales, L. Saviot, E. Duval, M. Gaudry, E. Cottancin, M. Pellarin, J. Lermé, M. Broyer, *Phys. Rev. B*, 2002, **65**, 165422(1-5).
7. S. Adichtchev, S. Sirotkin, G. Bachelier, L. Saviot, S. Etienne, B. Stephanidis, E. Duval and A. Mermet, *Phys. Rev. B*, 2009, **79**, 201402(R)(1-4).
8. H. K. Yadav, V. Gupta, K. Sreenivas, S. P. Singh, B. Sundarakannan and R. S. Katiyar, *Phys. Rev. Lett.*, 2006, **97**, 085502(1-4).
9. F. Calvo, *J. Phys. Chem. C*, 2011, **115**, 17730. *ibid*. 2012, **116**, 7607.
10. H. E. Sauceda and I. L. Garzón, *J. Phys. Chem. C*, 2015, dx.doi.org/10.1021/jp510666v.
11. M. Bayle, N. Combe, N. M. Sangeetha, G. Viau and R. Carles, *Nanoscale*, 2014, **6**, 9157.

12. M. Bayle, P. Benzo, N. Combe, C. Gatel, C. Bonafos, G. Benassayag and R. Carles, *Phys. Rev. B*, 2014, **89**, 195402(1-9).
13. H. E. Sauceda, D. Mongin, P. Maioli, A. Crut, M. Pellarin, N. Del Fatti, F. Vallée and I. L. Garzón, *J. Phys. Chem. C*, 2012, **116**, 25147.
14. H. E. Sauceda, F. Salazar, L. A. Pérez and I. L. Garzón, *J. Phys. Chem. C*, 2013, **117**, 25160.
15. V. Juvé, A. Crut, P. Maioli, M. Pellarin, M. Broyer, N. Del Fatti and F. Vallée, *Nano Lett.* 2010, **10**, 1853.
16. H. E. Sauceda, J. J. Pelayo, F. Salazar, L. A. Pérez and I. L. Garzón, *J. Phys. Chem. C*, 2013, **117**, 11393.
17. J. H. Hodak, A. Hengglein, M. Giersig and G. V. Hartland, *J. Phys. Chem. B*, 2000, **104**, 11708.
18. J. P. Wilcoxon, P. P. Provencio, *J. Am. Chem. Soc.*, 2004, **126**, 6402.
19. J. Zhu, Y.-C. Wang, L.-Q. Huang, Y.-M. Lu, *Phys. Lett. A* 2004, **323**, 455.
20. R. G. Sanedrin, D. G. Georganopoulou, S. Park, C. A. Mirkin, *Adv. Mater.*, 2005, **17**, 1027.
21. F. Hubenthal, T. Ziegler, C. Hendrich, M. Alschinger, F. Träger, *Eur. Phys. J. D*, 2005, **34**, 165.
22. R. P. Gupta, *Phys. Rev. B*, 1981, **23**, 6265.
23. V. Rosato, M. Guillopé, B. Legrand, *Philos. Mag. A*, 1989, **59**, 321.
24. F. Cleri and V. Rosato, *Phys. Rev. B*, 1993, **48**, 22.
25. A. Rapallo, G. Rossi, R. Ferrando, A. Fortunelli, B. C. Curley, L. D. Lloyd, G. M. Tarbuck, R. L. Johnston, *J. Chem. Phys.*, 2005, **122**, 194308.
26. G. Rossi, R. Ferrando, A. Rapallo, A. Fortunelli, B. C. Curley, L. D. Lloyd, R. L. Johnston, *J. Chem. Phys.*, 2005, **122**, 194309.
27. B. C. Curley, R. L. Johnston, G. Rossi, R. Ferrando, *Eur. Phys. J. D*, 2007, **43**,
28. L. O. Paz-Borbón, R. L. Johnston, G. Barcaro, A. Fortunelli, *J. Chem. Phys.*, 2008, **128**, 134517.
29. F. Chen and R. L. Johnston, *Acta Mater.,* 2008, **56**, 2374.
30. F. Chen and R. L. Johnston, *ACS Nano,* 2008, **2**, 165.
31. K. Michaelian, M. R. Beltrán, I. L. Garzón, *Phys. Rev. B*, 2002, **65**, 041403.
32. A. F. Jalbout, F. F. Contreras-Torres, L. A. Pérez, I. L. Garzón, *J. Phys. Chem. A*, 2008, **112**, 353.
33. I. E. Santizo, F. Hidalgo, L. A. Pérez, C. Noguez, I. L. Garzón, *J. Phys. Chem. C*, 2008, **112**, 17533.
34. H. Lei, J. Li., Y. Liu, X. Liu, *Eur. Phys. Lett.*, 2013, **101**, 46001.

Journal Name RSCPublishing

ARTICLE

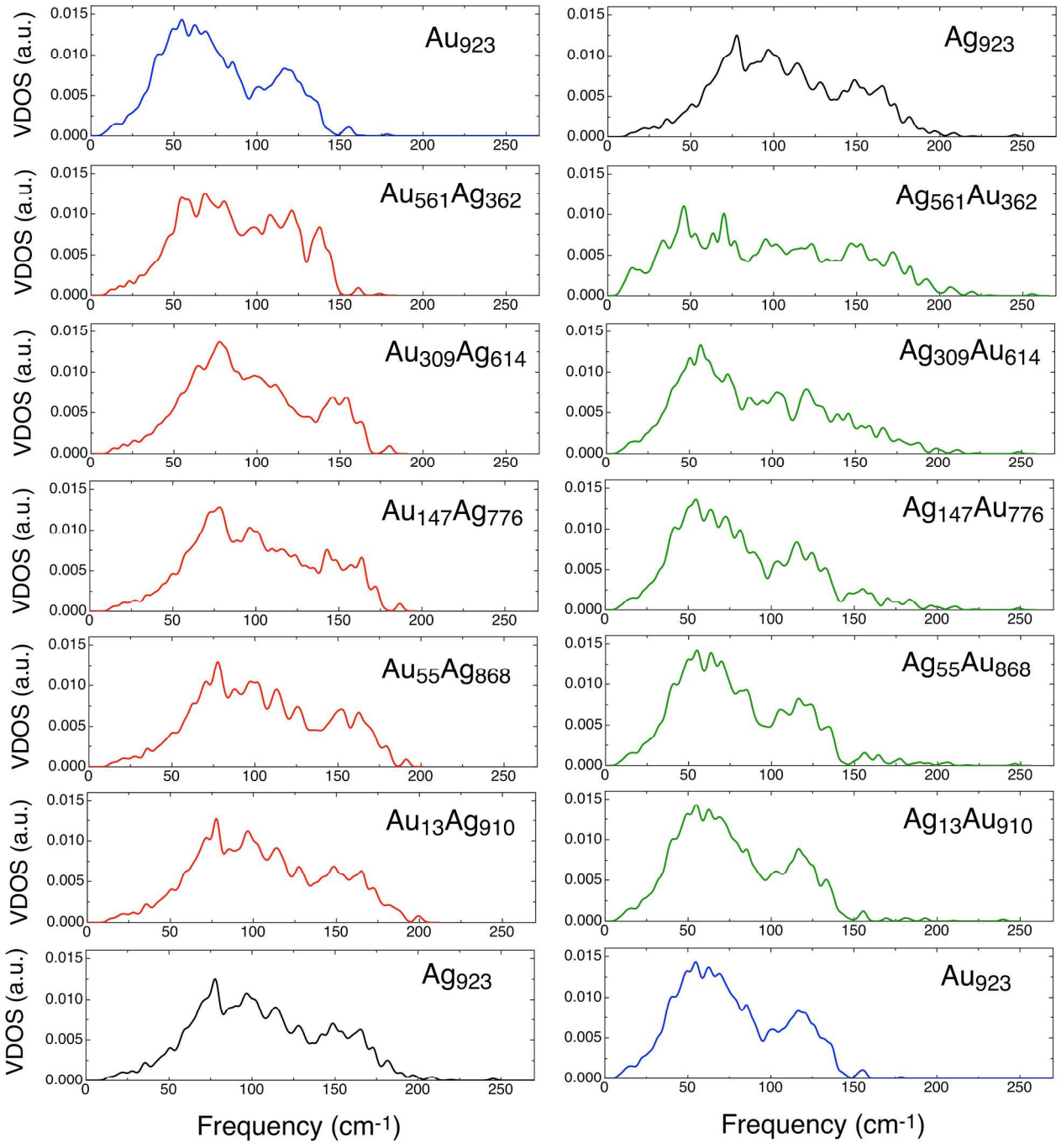

Figure 1. Vibrational density of states (VDOS) for the 923-atom bimetallic icosahedral Au_{core}-Ag_{shell} (left panels) and Ag_{core}-Au_{shell} (right panels) nanoparticles with different core-shell compositions. The VDOS for the pure Au_{923} and Ag_{923} icosahedral nanoparticles are also displayed for comparison.

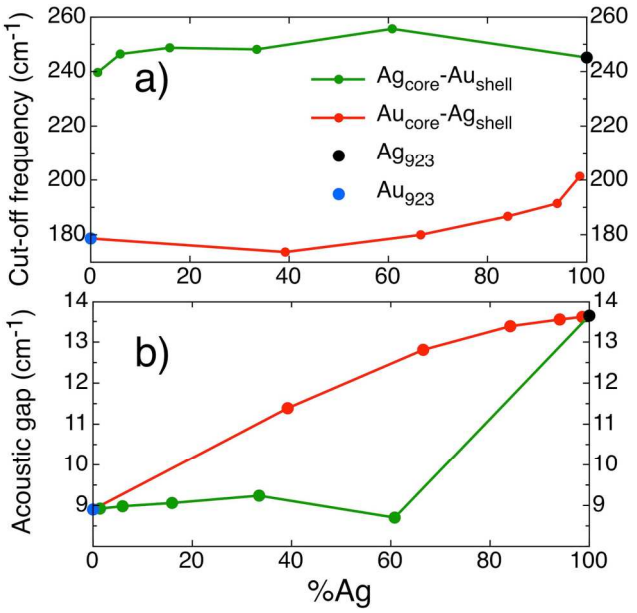

Figure 2. Cut-off (a) and acoustic gap (b) frequencies as a function of the percentage of Ag atomic composition for the 923-atom bimetallic icosahedral Au_{core}-Ag_{shell} (red points) and Ag_{core}-Au_{shell} (green points) nanoparticles with different core-shell compositions. Red (green) data points correspond to the compositions shown in the left (right) panels of Fig. 1.

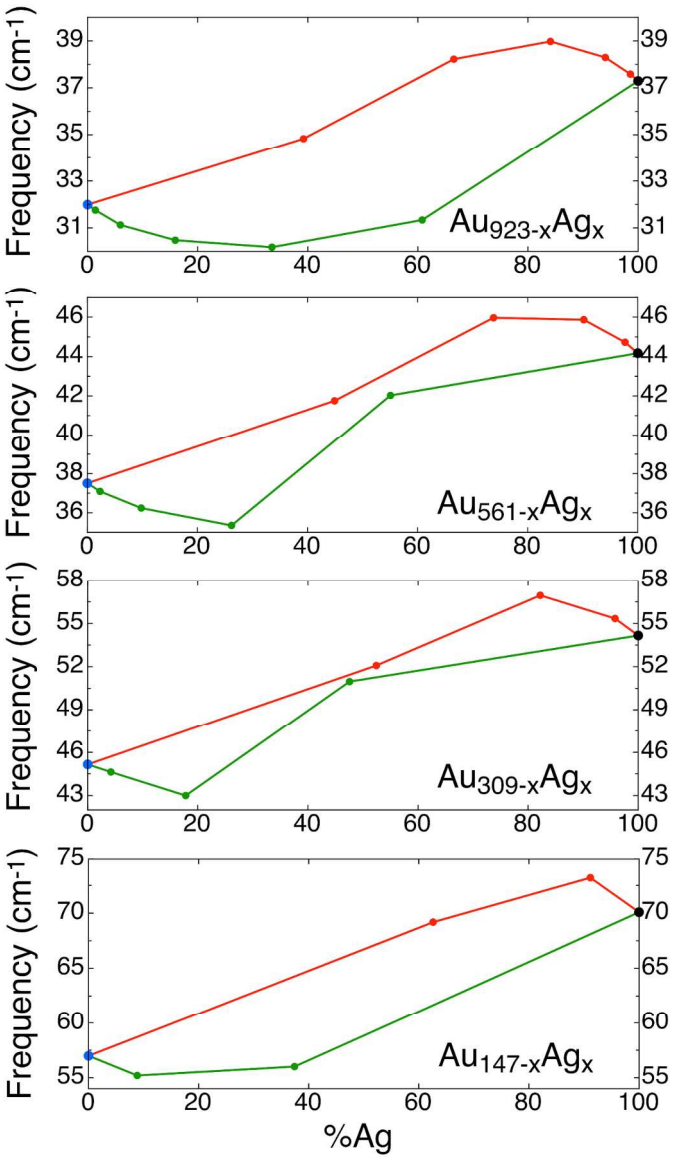

Figure 3. Quasi-breathing mode frequencies as a function of the percentage of Ag atomic composition for the 923-, 561-, 309-, and 147-atom bimetallic icosahedral Au_{core}-Ag_{shell} (red points) and Ag_{core}-Au_{shell} (green points) nanoparticles with different core-shell compositions. Red (green) data points correspond to the compositions shown in the left (right) panels of Fig. 1 (923), Fig. S1 (561), Fig. S2 (309), and Fig. S3 (147). Blue (black) dots correspond to the Au (Ag) pure nanoparticles.

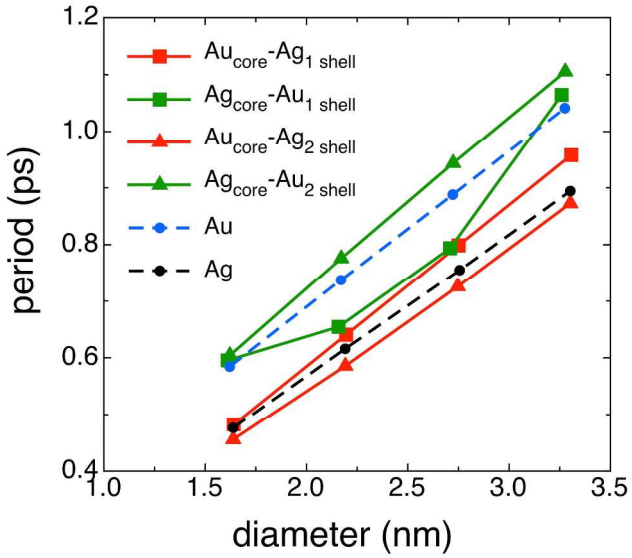

Figure 4. Quasi-breathing mode period as a function of size for bimetallic icosahedral Au_{core}-Ag_{shell} (red data) and Ag_{core}-Au_{shell} (green data) nanoparticles with one (squares) and two (triangles) shells. The nanoparticle compositions for growing sizes are : Red squares ($Au_{55}Ag_{92}$, $Au_{147}Ag_{162}$, $Au_{309}Ag_{252}$, $Au_{561}Ag_{362}$); red triangles ($Au_{13}Ag_{134}$, $Au_{55}Ag_{254}$, $Au_{147}Ag_{414}$, $Au_{309}Ag_{614}$); green squares ($Ag_{55}Au_{92}$, $Ag_{147}Au_{162}$, $Ag_{309}Au_{252}$, $Ag_{561}Au_{362}$); green triangles ($Ag_{13}Au_{134}$, $Ag_{55}Au_{254}$, $Ag_{147}Au_{414}$, $Ag_{309}Au_{614}$). The sizes for pure nanoparticles (blue and black points) correspond to 147-, 309-, 561-, 923-atoms.

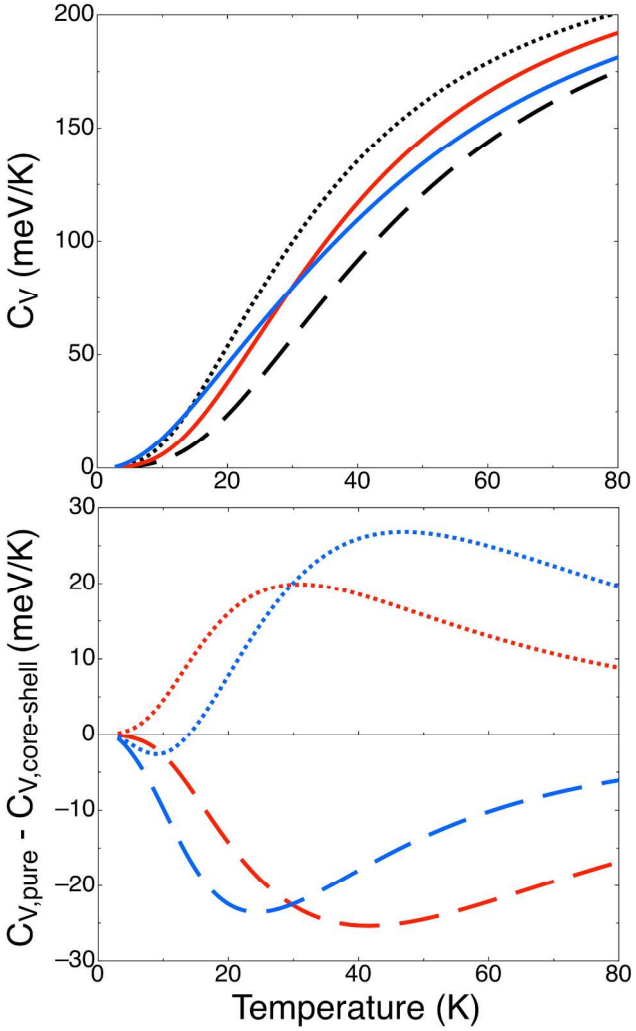

Figure 5. Low-temperature dependence of the specific heat of core-shell bimetallic icosahedral nanoparticles. Top panel: Pure Au_{923} (dotted line), $Au_{561}^{core}Ag_{362}^{shell}$ (red line), pure Ag_{923} (dashed line) and $Ag_{561}^{core}Au_{362}^{shell}$ (blue line). Bottom panel: Comparison of the specific heat between pure and bimetallic nanoparticles. Dotted lines correspond to the difference between Au_{923} and the two bimetallic nanoparticles. Dashed lines display the difference with respect to the Ag_{923} nanoparticle. It can be noticed the larger values of the $Ag_{561}^{core}Au_{362}^{shell}$ specific heat with respect to that one of Au_{923} in the temperature range 5-15 K.